Meso-scale modelling of concrete as a multiphase material

G. Xotta, V. Salomoni, C. Majorana, G. Mazzucco

Department of Structural and Transportation Engineering,
Faculty of Engineering, University of Padua, Italy
E-mail: xotta@dic.unipd.it, salomoni@unipd.it, majorana@.unipd.it, mazzucco@dic.unipd.it

Keywords: Concrete, composite material, meso-level, thermo-hygro-mechanical behaviour.

SUMMARY. Concrete is treated as a multiphase system, made of aggregates, interfacial transition zone (ITZ) and cement paste, modeled by means of a fully coupled three-dimensional FE code named NEWCON3D. The effects of the interface on the hygro-thermo mechanical response of concrete samples are analyzed.

1 INTRODUCTION

Concrete has a highly heterogeneous microstructure and its composite behaviour is exceedingly complex. For obtaining a deeper understanding and deducing the macroscopic constitutive behaviour of concrete, theoretical studies based on micromechanical analysis of the interaction between various components of concrete have been developed. However, the microstructure and properties of the individual components of concrete and their effects on the macroscopic material behaviour have not been yet fully understood. For such details to be included into the computational analysis, concrete needs to be analyzed as a multi-scale composite material where the microstructure would be realistically simulated [1, 2]. Even if in the numerical simulation of concrete at a mesoscopic level several parameters such as shape, size and distribution of coarse aggregates within the cement paste matrix significantly influence the mechanical behaviour of concrete, they will not be investigated in this article, being the objective that of focusing on the general potentialities of such an approach for better understanding specific phenomena in concrete, especially those where aggregate content is important, (e.g. spalling).

As a composite material, concrete is a mixture of cement paste with aggregates inclusions of different size [3]. The components of the heterogeneous material have different properties. The way they change with loading varies too. Variation in stiffness and strength of the components has influence on the global stiffness and fracture behaviour of the whole material. Different thermal expansion coefficients of the components result in internal stresses (eigenstresses) in the material when the global temperature changes. In this respect also heat of hydration during hardening and temperature changes during a fire are important aspects. Differences in porosity of the components influences mass transport and with that also hygral dilation. Different chemical compositions have influence on internal reactions taking place inside the material, which can also be a function of ingress of species [4].

The basic properties of the concrete are already formed during the development of the microstructure when the concrete hardens. During the lifetime of the structure these properties will change due to the impact of various mechanisms. Due to wall effects, large particles will not be present at the surface, and also temperature and moisture variations during hardening will influence the formation of the microstructure in the cover zone. As a result, the properties of the concrete in the cover zone and in the core of a structure are completely different. The concrete

properties are also function of water–cement ratio (w/c): lower w/c gives higher stiffness and strength. On the other hand, it also leads to more internal shrinkage.

In the multi-phase concrete material it has been found that the presence of the aggregates in the paste causes a thin layer of matrix material surrounding each inclusion to be more porous than the bulk of the surrounding cement paste matrix. This layer is called the interfacial transition zone (ITZ) [5-10], which is known to play an important role in the properties of a concrete composite [11, 12]. The ITZ has a layered structure, a lower density than the bulk matrix and is more penetrable by fluids and gases [13, 14]; therefore, the ITZ greatly influence the overall permeability of concrete [15]. Additionally, due to its complex structure, the ITZ appears to be the weakest region of the composite material when exposed to external loads [16]. Experiments demonstrated that the elastic modulus of concrete is strictly related to the elastic modulus and volume fraction of the ITZ regions [17, 18]. However, in the presence of low w/c ratios and/or fine mineral admixtures (e.g. silica fume), the ITZ may be absent or difficult to detect. Therefore, the ITZ is not necessarily an intrinsic feature of concrete, but will depend on factors such as the presence of admixtures, the type of mixing, w/c ratio, etc. [19].

When fracturing multi-phase materials like concrete a quasi-brittle behaviour is observed. In continuum mechanics, often concrete is schematised as a material showing a softening behaviour. Experimental studies have shown that if we zoom in on the material, we can explain why it is shown a softening behaviour. A zone of microcracks is formed and crack bridging, branching and friction effects all have a contribution to the toughness of concrete. The microstructure of the material has a large influence on the crack patterns in concrete. Cracks follow the weakest link in the material which is often the ITZ [20]. Transport of gases, moisture and ions takes place through the pore structure of concrete. Also transport follows the easiest route through the microstructure. Larger porosity in the ITZ and also cracks will increase this transport [4].

To describe the behaviour of concrete as a composite material, the F.E. NEWCON3D code, able to perform fully coupled hygro-thermo-mechanical analyses, was used. By means of this model, concrete can be treated as a multiphase systems, made of aggregates, ITZ and cement paste, where the voids of the solid skeleton are partly filled with liquid and partly with gas. As regards the mechanical field, NEWCON3D incorporates coupled thermal, creep and shrinkage effects as well as coupled damage and plasticity effects under medium and high temperature levels. Particularly the adopted damage model is a scalar isotropic one.

As a first numerical example [21] it is considered in the following a cubic concrete sample of $100\times100\times100$ mm^3 with a symmetric distribution of aggregates of different sizes and without ITZ. The sample is supposed to be initially close to a saturated state with (dry) aggregates surrounded by cement paste and heated, on each side, up to 50°C. Subsequently, a second cubic sample with a more refined discretization and the presence of ITZ is analyzed in detail.

2 THE MATHEMATICAL MODEL

Concrete is treated as a multiphase system where the voids of the skeleton are partly filled with liquid and partly with a gas phase [22, 23]. The liquid phase consists of bound water (or adsorbed water), which is present in the whole range of water contents of the medium, and capillary water (or free water), which appears when water content exceeds so-called solid saturation point S_{ssp} [24], i.e. the upper limit of the hygroscopic region of moisture content. The gas phase, i.e. moist air, is a mixture of dry air (non-condensable constituent) and water vapour (condensable gas), and it is assumed to behave as an ideal gas.

The approach here is to start from a phenomenological model, originally developed by Bažant and co-authors, in which mass diffusion and heat convection-conduction equations are written in

terms of relative humidity, to an upgraded version in which its non-linear diffusive nature is maintained as well as the substitution of the linear momentum balance equations of the fluids with a constitutive equation for fluxes; moreover new calculations of thermodynamic properties for gaseous phases are implemented to include high ranges of both pressure and temperature. Additionally, Darcy's law is modified when describing gas flow through concrete. The proposed model couples non-linear material relations with experimental relations; to enhance its predictive capabilities, a predictor-corrector procedure is supplemented to enhance the convergence of the solution. For details about the PC scheme, as well as the field equations for the coupled heat and mass transfer in concrete, the reader is referred to [21, 25].

As regards the mechanical field, NEWCON3D couples shrinkage, creep, damage and plasticity effects under medium and high temperature levels.

2.1 *The mechanical field*

The constitutive relationship for the solid skeleton in incremental form can be written as

$$d\boldsymbol{\sigma}' = (1-D)\mathbf{D}_T(d\boldsymbol{\varepsilon} - d\boldsymbol{\varepsilon}_T - d\boldsymbol{\varepsilon}_c - d\boldsymbol{\varepsilon}_{lits} - d\boldsymbol{\varepsilon}_p - d\boldsymbol{\varepsilon}_{sh} - d\boldsymbol{\varepsilon}_0) \tag{1}$$

where $\boldsymbol{\sigma}'$ is the effective stress, $\mathbf{D}_T$ is the tangent stiffness matrix, D is the chemo-thermo-mechanical damage, $d\boldsymbol{\varepsilon}_T$ is the strain rate caused by thermo-elastic expansion, $d\boldsymbol{\varepsilon}_c$ is the strain rate accounting for creep, $d\boldsymbol{\varepsilon}_{lits}$ is *the load induced thermal strain rate*, $d\boldsymbol{\varepsilon}_p$ is the plastic strain rate, $d\boldsymbol{\varepsilon}_{sh}$ is due to shrinkage and $d\boldsymbol{\varepsilon}_0$ represents the autogeneous strain increments (e.g. due to chemical variations) and the irreversible part of the strain rates not contained in the previous terms.

Considering the effective stress definition, the macroscopic *linear momentum balance equation* for the whole medium may be expressed in the form

$$div(\boldsymbol{\sigma}' + p\mathbf{I}) + [(1-\varphi)\rho_s + \varphi S_w\rho_w + \varphi(1 - S_w)\rho_g]\mathbf{g} = 0 \tag{2}$$

with $\varphi = \varphi(T)$, [17]. As regards the creep and shrinkage effects as well as coupled damage and plasticity effects under medium and high temperature levels the reader is referred to [21, 26, 27, 28].

2.2 *Finite Element Discretization*

The application, within the numerical code NEWCON3D, of a standard finite element discretization in space of the *linear momentum, mass transfer and heat balance equations*, results in [30, 31, 32, 23, 29]

$$\begin{bmatrix} \mathbf{K} & \mathbf{HU} & \mathbf{TU} \\ \mathbf{L}^T & \mathbf{I} & \mathbf{TP} \\ \mathbf{0} & \mathbf{TH} & \mathbf{TS} \end{bmatrix} \begin{Bmatrix} \dot{\overline{\mathbf{u}}} \\ \dot{\overline{\mathbf{h}}} \\ \dot{\overline{\mathbf{T}}} \end{Bmatrix} + \begin{bmatrix} \mathbf{0} & \mathbf{0} & \mathbf{0} \\ \mathbf{0} & \mathbf{Q} & \mathbf{0} \\ \mathbf{0} & \mathbf{0} & \mathbf{TR} \end{bmatrix} \begin{Bmatrix} \overline{\mathbf{u}} \\ \overline{\mathbf{h}} \\ \overline{\mathbf{T}} \end{Bmatrix} = \begin{Bmatrix} \dot{\mathbf{f}} + \mathbf{c} \\ \dot{\mathbf{HG}} \\ \dot{\mathbf{TG}} \end{Bmatrix} \tag{3}$$

in which $\overline{\mathbf{u}}$, $\overline{\mathbf{h}}$ and $\overline{\mathbf{T}}$ are the nodal values of the basic variables; the matrices in eq. (3) take the form reported in *Appendix I*.

3 NUMERICAL ANALYSES

The first numerical analysis presented here is referred to a cubic concrete sample of

100×100×100 mm^3 without ITZ and with a symmetric (for sake of simplicity) distribution of aggregates (Figure 1), as e.g. in [1]. As previously mentioned in the introduction, the sample has been supposed to be initially close to a saturated state, with (dry) aggregates fully surrounded by cement paste, and submited to a temperature of 50°C on each external face. Only after 33 minutes the sample results completely heated (Figure 2) while, as regards the relative humidity, it is partially saturated even after 3 days (Figure 3). The relative humidity and temperature distribution of three representative nodes (one node inside the aggregate, one on the interface between cement paste and aggregate and the last one in the cement paste) are reported in Figure 4.

As regards the temperature behavior the aggregates have an higher thermal conductivity compared to that of the cement paste, hence the temperature increases slightly more rapidly in the aggregates, inducing the interface to desaturate and causing thermo-diffusion of water vapour towards the colder zones. On the other side, in correspondence of the interface there is a first evident increase in humidity (this is caused by the presence of aggregates that constitute a physical obstacle to humidity fluxes) accompanied by a decrease in the cement paste (this is due to thermal gradients). Then, before reaching equilibrium, the situation is reversed and humidity flows tend to become equally distributed between the aggregates surface and the cement paste.

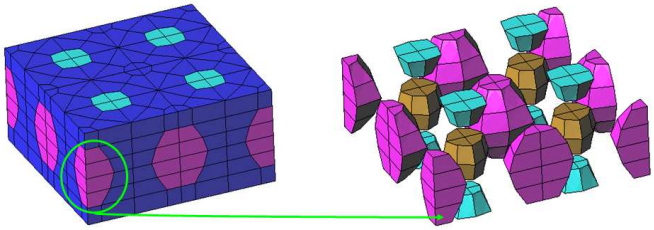

Figure 1: Adopted discretization for the meso-scale analysis without ITZ (half sample).

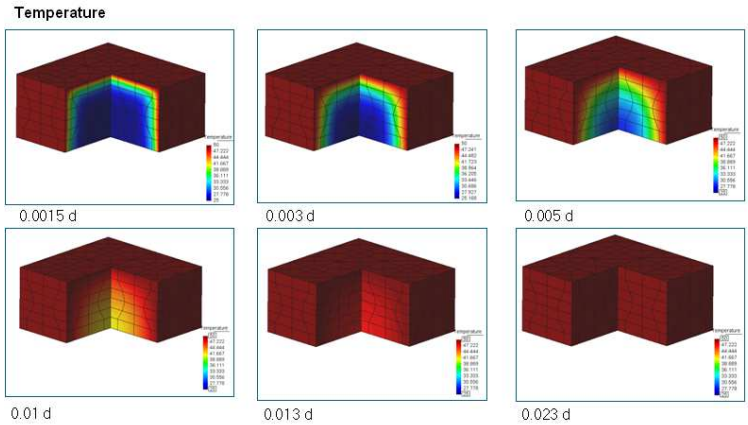

Figure 2: Evolution of temperature on the half meso-scale concrete sample.

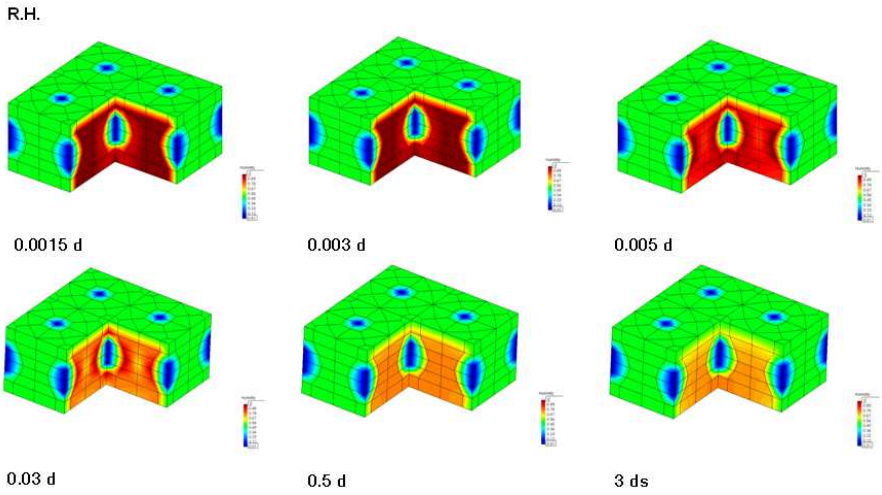

Figure 3: Evolution of R.H. on the half meso-scale concrete sample.

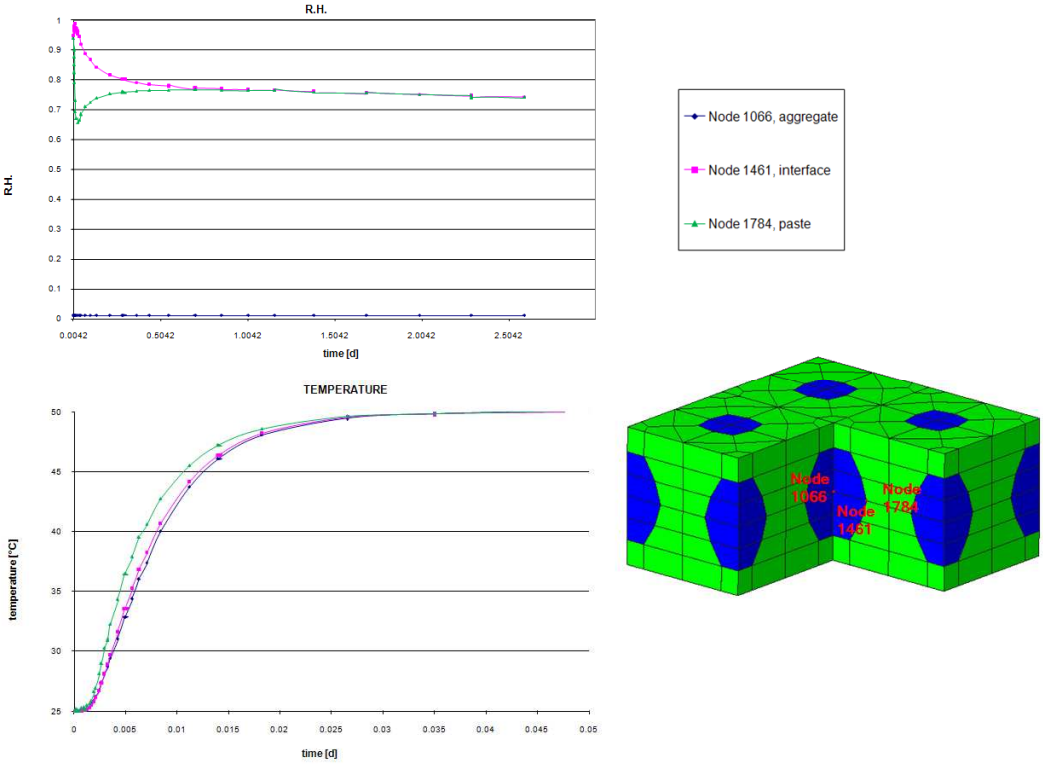

Figure 4: R.H. and temperature distribution between aggregate and cement paste (half sample).

The second numerical example is related to another cubic concrete sample of 100×100×100 mm^3 with a symmetric distribution of aggregates of different sizes, a more refined mesh (928 20-node isoparametric element and 4625 nodes), and the presence of ITZ (Figure 5); in Table 1 the main material data for cement paste, ITZ and aggregates [1, 3, 6, 7, 10] are reported.

Again, the sample has been supposed to be initially close to a saturated state and heated on the external surfaces up to 50°C, but differently from the previous example the (dry) aggregates are fully surrounded by an interfacial transition zone (ITZ) of about 1 mm thickness. The presence of this zone influences the temperature and humidity fields because of its lower density and its higher porosity compared with that of the cement paste. Indeed the effect of ITZs is particularly evident on the sample's hygral state: differently from what shown in the previous analysis, a higher diffusivity of the ITZ pushes water flows towards the cement paste (hence increasing its saturation level). While as regards the temperature its maximum value is reached after 60 days.

As example, the chemo-thermo-mechanical damage is supposed to be triggered in the early stages of the analysis, first developing in the ITZ and at its interface with the cement paste; later on, due to essentially the restrained expansion of the internal part of the sample with the consequent development of tensile stresses, damage starts affecting there the cement paste. Damage due to compression is activated externally, and particularly in the ITZs surrounding the aggregates.

Table 1:Material data for the meso-scale analysis with ITZ.

properties	**cement paste**	**ITZ**	**aggregate**
Elastic modulus [MPa]	20000	10000	67000
Poisson's ratio	0.2	0.2	0.2
Reference diffusivity along x/y/z directions [mm^2/day]	40.	80.	0.
Unrestrained shrinkage for h = 0 (ε_{sh})	$-0.4\cdot10^{-3}$	$-0.4\cdot10^{-3}$	0.
Thermal expansion coefficient of solid	$0.12\cdot10^{-4}$	$0.4\cdot10^{-5}$	0.
Heat conductivity along x/y/z directions [N/(day K)]	$0.11\cdot10^{6}$	$0.22\cdot10^{6}$	$0.17\cdot10^{6}$
Initial damage coefficient	$0.1\cdot10^{-4}$	$0.1\cdot10^{-6}$	-
Coefficient A_t for damage in tension	1.2	1.2	-
Coefficient B_t for damage in tension	$5.0\cdot10^{3}$	$5.0\cdot10^{3}$	-
Coefficient A_c for damage in compression	1.0	1.0	-
Coefficient B_c for damage in compression	$0.1\cdot10^{4}$	$0.1\cdot10^{4}$	-
Characteristic length l_c	$0.6\cdot10^{2}$	$0.6\cdot10^{2}$	-

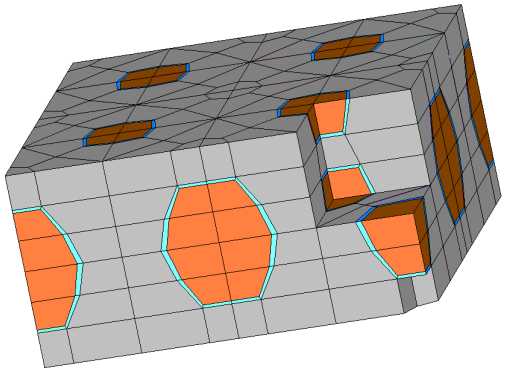

Figure 5: Adopted discretization for the meso-scale analysis with ITZ (half sample).

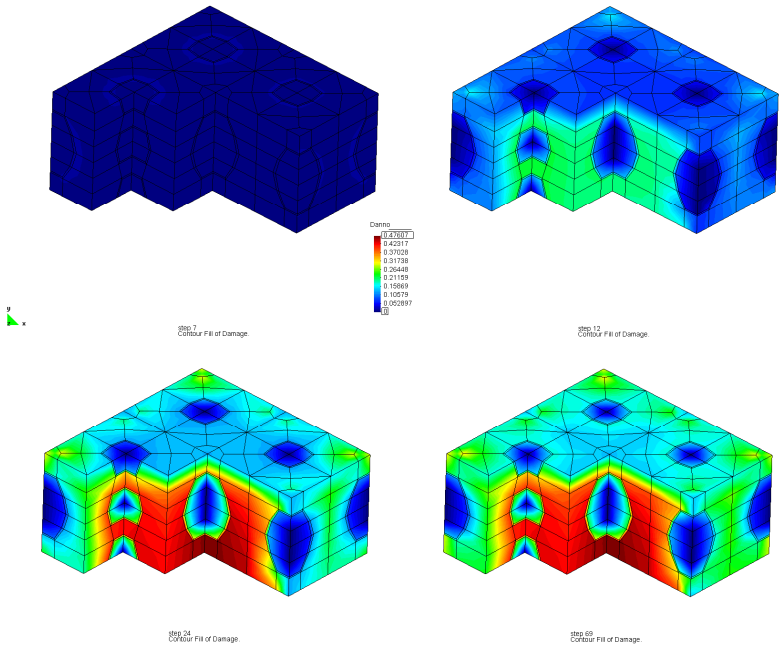

Figure 6: Evolution of damage on the half meso-scale concrete sample (with ITZ).

4 CONCLUSIONS

A chemo-thermo-hydro-mechanical multiphase model of concrete able to describe its behaviour at the meso-level under medium and high temperature ranges has been described, including the feature of the Interface Transition Zone (ITZ) .

The model incorporates coupled elastoplastic and damage behaviour plus creep effects. The stress–strain numerical model is derived according to thermodynamic consistency and is based on experimental findings. Such fundamental issue is properly included in a chemo-thermo-hydro-mechanical modelling of concrete at low to medium as well as high temperature ranges. For heat

and mass transport purposes, several approaches can be used at macro or meso-levels. Aggregates and cement matrix are usually smeared (at macrolevel), but fluids can be separated or not, giving rise to different degrees of insight in the heat and mass behaviour. However, for computational purposes both are used in the scientific community, due also to calculation time needed and available computer power. Also the separation of aggregate from matrix, needed for fully understanding and predicting spalling behavior of concrete, is becoming more affordable, as far as 3D parallel computation will become economically feasible. Full description of phase changes, sorption-desorption behaviour at high temperature/fire and related strains are progressively achieved in the analysis.

From the mechanical point of view, the stress-strain constitutive relationship for concrete under high temperature and fire needs to take into account several effects like thermal, shrinkage, creep, LITS, damage, plastic and other chemical contributions that must be carefully checked against experiments, if a meso-level analysis and ITZ would be included.

Appendix I

The matrices in eq. (3) are defined as reported below:

$$
\begin{aligned}
\mathbf{K} &= -\int_{\Omega} \mathbf{B}^T \mathbf{D}_T \mathbf{B} d\Omega \\
\mathbf{HU} &= \int_{\Omega} \mathbf{B}^T \mathbf{D}_T \boldsymbol{\kappa} \mathbf{N} d\Omega \\
\mathbf{TU} &= \int_{\Omega} \mathbf{B}^T \mathbf{D}_T \boldsymbol{\alpha} \mathbf{N} d\Omega \\
\mathbf{L}^T &= \int_{\Omega} \mathbf{N}^T \mathbf{m}^T \chi \mathbf{B} d\Omega \\
\mathbf{TP} &= -\int_{\Omega} \mathbf{N}^T k \mathbf{N} d\Omega \\
\mathbf{Q} &= \int_{\Omega} (\nabla \mathbf{N})^T \mathbf{C} (\nabla \mathbf{N}) d\Omega \\
\mathbf{TH} &= \int_{\Omega} \mathbf{N}^T \left((1-\phi) C_s \frac{\rho_s}{k_s} + \phi C_{moist} \frac{\rho_{moist}}{k_{moist}} \right) \mathbf{N} \overline{\mathbf{T}} \mathbf{N} p_{gws} d\Omega \\
\mathbf{TS} &= \int_{\Omega} \mathbf{N}^T \rho C_q \mathbf{N} d\Omega \\
\mathbf{TR} &= \int_{\Omega} (\nabla \mathbf{N})^T \boldsymbol{\Lambda} (\nabla \mathbf{N}) d\Omega - \int_{\Omega} (\nabla \mathbf{N})^T \rho_{moist} C_{moist} \mathbf{V}_h \mathbf{N} d\Omega
\end{aligned}
\tag{A1}
$$

$$
\begin{aligned}
\mathbf{c} &= -\int_{\Omega} \mathbf{B}^T \mathbf{D}_T \mathbf{D}_T^{-1} \sum_{\mu=1}^{N} \frac{\varphi_T \varphi_h}{\tau_\mu} \boldsymbol{\sigma}_\mu d\Omega \\
d\mathbf{f} &= -\int_{\Omega} \mathbf{N}^T d\mathbf{b} d\Omega - \int_{\Gamma} \mathbf{N}^T d\hat{\mathbf{t}} d\Gamma - \int_{\Omega} \mathbf{B}^T \mathbf{D}_T d\boldsymbol{\varepsilon}_0 d\Omega \\
\mathbf{HG} &= \int_{\Omega} \mathbf{N}^T h_s d\Omega \\
\mathbf{TG} &= -\int_{\Omega} \mathbf{N}^T Q_h \mathbf{N} d\Omega - \int_{\Gamma} \mathbf{N}^T q_h d\Gamma
\end{aligned}
\tag{A2}
$$

In eqs. (A1) and (A2) **HU** and **TU** account for shrinkage and thermal dilation effects, respectively; $\mathbf{L}^T$ and **TP** are the coupling matrices representing the influence of the mechanical and thermal field on the hygral one, respectively; **Q** is the diffusivity matrix accounting also for sorption-desorption isotherms; **TH** the coupling matrix between the hygral and thermal fields in terms of capacity; **TS** the matrix of heat capacity; **TR** the matrix of thermal transmission including the convective term; **c** the matrix accounting for creep; **HG** the matrix of humidity variation due to drying and **TG** accounts for heat fluxes. For further explanations of the above terms the reader is referred to [30, 31, 32, 23, 29].

References

[1] Wriggers, P., Moftah, S.O., "Mesoscale models for concrete: Homogenisation and damage behaviour," in *Finite El An Des*, **42**, 623-636 (2006).

[2] Dupray, F, Malecot, Y., Daudeville, L. and Buzaud, E., "A mesoscopic model for the behaviour of concrete under high confinement," in *Int. J. Numer. Anal. Meth. Geomech.*, **33**, 1407-1423, (2009).

[3] Sun, Z., Garboczi, E.J., Shah, S.P., "Modeling the elastic properties of concrete composites: Experiment, differential effective medium theory, and numerical simulation," in *Cem Con Comp*, **29**, 22-38 (2007).

[4] Schlangen, E., Koenders, E.A.B. and van Breugel, K., "Influence of internal dilation on the fracture behaviour of multi-phase materials," in *Engrg Frac Mech*, **74**, 18-33 (2007).

[5] Scrivener, K.L., "The microstructure of concrete," in *Material science of concrete*, **1**, 127-62 (1989)

[6] Scrivener, K.L., Pratt, P.L., "Characterization of interfacial microstructure," in *Interfacial transition zone in concrete*, (RILEM Report 11, London, UK), 3-17 (1996).

[7] Scrivener, K.L., "Characterization of the ITZ and its quantification by test methods," in *Engineering and transport properties of the interfacial transition zone in cementitious composites*, (RILEM Report 20, RILEM Publications S.A.R.L., France), 3-15 (1999).

[8] Scrivener, K.L., Nemati, K.M., "The percolation of pore space in the cement paste/aggregate interfacial zone of concrete," in *Cem Conc Res*, ***26*(1)**, 35–40 (1996).

[9] Bentz, D.P., Garboczi, E.J., Stutzman, P.E., "Computer modeling of the interfacial transition zone in concrete," in *Interfaces in cementitious composites*, 259–68 (1993).

[10] Bentz, D.P., Stutzman, P.A., Garboczi, E.J., "Experimental and simulation studies of the interfacial zone in concrete," in *Cem Conc Res.*, ***22*(5)**, 891–902 (1992).

[11] Scrivener, K.L., Gariner, E.M., "Microstructural gradients in cement paste around aggregate particles," in *Bonding in cementitious composites*, (Mindess S., Shah S.P., Eds.), **114**, 77-85.

[12] Prokopski, G., Halbiniak, J., "Interfacial transition zone in cementitious materials," in *Cem Con Res*, **30(4)**, 579–83 (2000).

[13] Liao, K.Y., Chang, P.K., Peng, Y.N., Yang, C.C., "A study on characteristics of interfacial transition zone in concrete," in *Cem Con Res*, **34(6)**, 977-89 (2004).

[14] Ollivier, J.P., Maso, J.C., Bourdette, B., "Interfacial Transition Zone in Concrete," in *Advn Cem Bas Mat*, **2**, 30-38 (1995).

[15] Garboczi, E.J., Bentz, D.P., Schwartz L.M., "Modeling the influence of the interfacial zone on the D.C. electrical conductivity of mortar," in *Adv. Cement-Based Mater*, ***2*(5)**, 169–81 (1995).

[16] Brandt, A.M., "Cement-based composites: materials, mechanical properties and performance," (E&FN Spon: London, UK), (1995).

[17] Simeonov, P., Ahmad, S., "Effect of transition zone on the elastic behavior of cement-based composites," in *Cem Conc Res*, **25(1)**, 165–76 (1995).
[18] Zheng, J.J., Zhou, X.Z., "A numerical method for predicting the elastic modulus of concrete made with two different aggregates," in *J Zhejiang Univ SCIENCE A*, ***7*(II)**, 293-296, (2006).
[19] Garboczi, E.J., Bentz, D.P., Shane, J.D., "Effect of the interfacial zone on the conductivity of Portland cement mortars," in *J Am Cer Soc*., ***83*(5)**, 1137-1144, (2000).
[20] Caballero, A., Lopez, C.M., Carol, I., "3D meso-structural analysis of concrete specimens under uniaxial tension," in *Comp Meth Appl Mech Engrg*, **195**, 7182-7195, (2006).
[21] Salomoni, V., Majorana, C., Mazzucco, G., Xotta, G., Khoury, G.A., "Multiscale modelling of Concrete as a Fully Coupled Porous Medium," in *Concrete Materials: Properties, Performance and Applications*, Ch.3, NOVA Publishers, 2009 (in press), (ISBN: 978-1-60741-250-2).
[22] Gawin, D., Majorana, C.E., Schrefler, B.A., "Numerical analysis of hygro-thermal behaviour and damage of concrete at high temperature," in *Mech Coh Frict Mat* , **4**, 37-74 (1999).
[23] Baggio, P., Majorana, C.E., Schrefler, B.A., "Thermo-hygro-mechanical analysis of concrete," in *Int J Num Meth Fluids*, *20*, 573-595 (1995).
[24] Couture, F., Jomaa, W., Ruiggali, J.R., "Relative permeability relations: a key factor for a drying model.," in *Tran Por Media*, **23**, 303-335 (1996).
[25] Salomoni, V.A., Majorana, C.E., Giannuzzi, G.M., Miliozzi, A., "Thermal-fluid flow within innovative heat storage concrete systems for solar power plants.," in *Int J Num Meth Heat Fluid Flow*, (Special Issue), **18**(7/8), 969-999, (2008).
[26] Majorana, C.E., Salomoni, V.A., Khoury, G.A., "Micro-structural modeling of concrete under fire conditions," in (Rodrigues, Khoury, Høj (Eds.)), *Proc. Int. Workshop Fire Design of Concrete Structures – From materials modeling to structural performance*, 81-94, (2007).
[27] Salomoni, V.A., Majorana, C.E., Khoury, G.A., "Stress-strain experimental-based modeling of concrete under high temperature conditions", in (B.H.V. Topping (Ed.)) *Civil Engineering Computations: Tools and Techniques*, Ch.**14**, (Saxe-Coburg Publications), 319-346, (2007).
[28] Salomoni, V.A., Majorana, C.E., Khoury, G.A., "Strain modelling of heated concrete," in (Tanabe-Sokata-Mihashi-Sato-Maekawa-Nakamura (Eds.)) *Proc. CONCREEP8 - 8th Int. Conf. on Creep, Shrinkage and Durability of Concrete and Concrete Structures*, **II**, 1005-1011, (2008).
[29] Majorana, C.E., Salomoni, V., Schrefler, B.A., "Hygrothermal and mechanical model of concrete at high temperature," in *Mat Struc*, **31(210)**, 378-386 (1998).
[30] Lewis, R.W., Schrefler, B.A., "The Finite Element Method in the Deformation and Consolidation of Porous Media," (J. Wiley, Chichester), (1987).
[31] Schrefler, B.A., Simoni, L., Majorana, C.E., "A general model for the mechanics of saturated-unsaturated porous materials," in *Mat Str*, **22**, 323-334 (1989).
[32] Lewis, R.W., Schrefler, B.A., "The Finite Element Method in the Static and Dynamic Deformation and Consolidation of Porous Media," (John Wiley & Sons: Chichester, UK), (1998).